Structures And Magnetization Of Defect-Associated Sites In Silicon

L. Chow[a], J. C. Gonzalez-Pons[a], E. del Barco[a], R. Vanfleet[b], A. Misiuk[c], A. Barcz[c,d], E. S. Choi[e], and G. Chai[f]

[a]*Department of Physics, University of Central Florida, Orlando, FL 32816-2385 USA*
[b]*Department of Physics, Brigham Young University, Provo, UT 84602 USA*
[c]*Institute of Electron Technology (ITE), al. Lotnikow 32/46, Warsaw 02-668 Poland*
[d]*Polish Academy of Science, Institute of Physics, al Lotnikow 32/46, Warsaw 02-668 Poland*
[e]*NHMFL, Florida State University, Tallahassee, FL 32310-3706 USA*
[f]*Apollo Technologies, Inc. 205 Waymont Court, Suite 111, Lake Mary, FL 32746 USA*

Abstract. To better understand the mechanism of the reported "quasi-ferromagnetism" observed in Si ions self-implanted or irradiated silicon, we carry out high resolution transmission electron microscopy (HRTEM), magnetization measurements using superconducting quantum interference device (SQUID) magnetometer, and ferromagnetic resonance (FMR) measurements of the magnetic interaction of the defect-associated sites in silicon damaged by silicon self-implantation or energetic particle beams. The SQUID measurements showed that the silicon self-implanted sample has paramagnetic ordering. FMR measurements indicated the He^{++} irradiated sample has a ferromagnetic interaction and yields a Lande g-factor of 2.35.

Keywords: Si, ion implantation, transmission electron microscopy, ferromagnetic resonance.
PACS: 61.72.-y, 61.80.-x, 66.30.Ny, 75.50.Pp, 76.50.+g.

INTRODUCTION

Recently, ferromagnetic hysteresis loop has been observed at room temperature in single crystalline silicon substrates implanted with a dose of 1×10^{16} cm^{-2} of Si ions or 2×10^{16} cm^{-2} of Ar ions, and in silicon wafers irradiated with a dose of 4×10^{16} cm^{-2} of thermal neutron flux [1]. It has been suggested that the paramagnetic defects, i.e., the unpaired spins of dangling bonds created during the implantation or irradiation process interact to yield the quasi-ferromagnetism observed in defect or damage associated silicon [2]. These results could have important implications on the magnetic behavior of transition metals implanted silicon substrates [3-6].

The appearance of ferromagnetic ordering in silicon implanted with low energy Ar and Ne ions at low temperature have been reported 30 years ago [7]. More recently Adashkevich et al. [8] have carried out FMR measurements on high energy Xe (5.68 GeV) and Kr (210 MeV) implanted silicon samples. In addition to a number of well known EPR lines associated with point defects in silicon, they found a broad magnetic resonance line with a g-factor of 2.2 for Kr and a g-factor of 3.4 for Xe^{+} implanted silicon samples. The authors attributed the broad magnetic resonance lines (g = 2.2 or 3.4) to the formation of regions with different degree of magnetic order as a result of

CP1003, *Magnetic Materials, International Conference on Magnetic Materials (ICMM-2007)*
edited by A. Ghoshray and B. Bandyopadhyay

high energy implantation. They believe the signals come from the manifestation of internal magnetic fields from inclusions with high concentration of unpaired electrons.

This "quasi-ferromagnetism" is not limited to the implanted silicon only. Both etched porous silicon [9] and spark-processed silicon [2] have shown magnetic hysteresis behavior in the past. Also, there is an extensive review [10] of ferromagnetic ordering in many allotropic forms of carbon including pyrolytic decomposition of polymers [11], protons irradiated graphite [12], fullerene films polymerized by pressure [13], and others.

We have investigated self-implanted silicon, and electron or neutron irradiated silicon using HRTEM, SQUID magnetometer and FMR measurements, to understand the origin and mechanism of magnetic ordering in defect-associated sites in silicon.

EXPERIMENTAL

Seven silicon samples have been studied. Two samples are irradiated with 2.5 MeV electrons at a flux of 1×10^{17} cm^{-2}. Sample E-1 is the as-irradiated and sample E-2 is annealed for one hour at 450 °C under one atmosphere of high purity Ar gas. The next three samples are implanted with 20 keV α particles at a flux of 1×10^{17} cm^{-2}. The implantation angle is 60° with respect to the normal of the substrate. Sample α-1 is as-implanted, sample α-2 is annealed for one hour at 450 °C and sample α-3 is annealed for 45 minutes at 300 °C. The last two samples are Si^{+} ions implanted silicon samples. Sample S-1 is a floating zone silicon (FzSi) with a <111> orientation and is as-implanted with Si ions with an energy of 150 keV at a dose of 2×10^{16} cm^{-2}. Sample S-2 is a Czochralski grown silicon implanted with 50 keV Si ions at a dose of 1×10^{17} cm^{-2} followed by annealing at 275 C and 10.5 kbar for 1.5 hours.

Magnetization measurements were carried out at 10 K using a commercial SQUID magnetometer (Quantum Design MPMS) on six samples (i.e., E-1, E-2, α-1, α-2, S-1 and S-2) with appropriate subtraction of the background signal. The samples were zero-field cooled and the field was applied parallel to the substrate surface.

Samples E-1 and S-1 were analyzed by TEM studies. The specimens were prepared in a cross sectional geometry by tripod polishing and viewed with Tecnai TF20 in both TEM and STEM modes.

FMR measurements were conducted at room temperature by employing a broad-band (f = 1-40 GHz) coplanar waveguide (CPW) in the transmission mode as an inductive sensor and a 1.4 Tesla electromagnet capable to rotate in a plane.

RESULTS

The magnetization behavior of S-1 and S-2 samples are shown in Fig. 1(a) and (b). Only S-1 sample showed a strong magnetic ordering at low temperature.

Figures 2(a) and (b) are TEM micrographs of sample S-1 showing the amorphous layer due to ion implantation. The end of range (EOR) defect is also clearly seen. The EOR defect thickness is about 60-80 nm which is narrower than the EOR region created by other impurity atoms implanted under similar conditions [15]. Figure 2(b) shows a closer look at the amorphous-crystalline boundary and EOR region. The E-1 sample showed no evidence of any damage in the silicon crystal structure.

FMR measurements showed evidence of ferromagnetic behavior at room temperature only in sample α-3. Note that this sample is intermediate between α-1 (as implanted) and α-2 (annealed at 450 ^{o}C for an hour), which showed no magnetic behavior at any temperature. A clear FMR signal is observed in the absorption

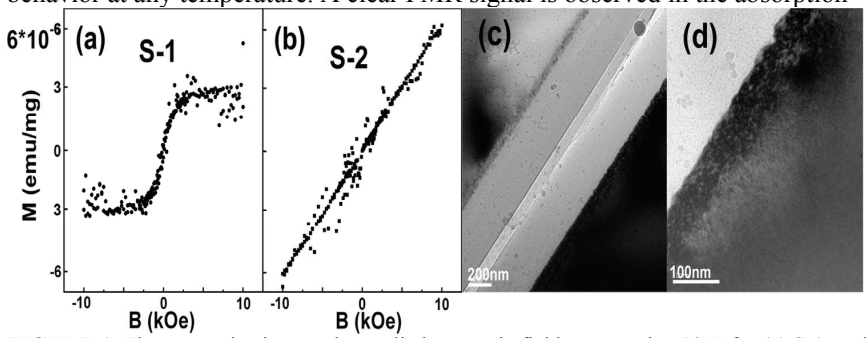

FIGURE 1. The magnetization vs. the applied magnetic field measured at 10 K for (a) S-1, and (b) S-2. TEM micrograph of sample S-1 (c) near the amorphous-crystalline boundary region, (d) higher magnification image at the a-c interface.

spectrum at 3.5 kG when 25 GHz microwaves are employed. The linewidth of this absorption line is quite broad at about 1.2 KG. Therefore, this is unlikely to be due to the EPR signal of a single electron in a dangling bond, where the linewidth is about a few Gauss. Observation of this broad peak indicates certain collective magnetic interactions existing in the sample. From our experience with the Mn implanted samples [15], we expected this collective magnetic interaction to be in a thin layer buried inside the silicon substrate, perhaps similar to the EOR defective layer observed in Fig. 2. Therefore we apply the magnetic field in the plane of the substrate, and measured the frequency dependency of the resonance field. Under this geometry, f^2/H vs. H should follow a straight line [16],

$$\left(\frac{f}{2\pi\gamma}\right)^2 = H_R(H_R + 4\pi M_{eff}) \qquad (1)$$

where the zero-field intercept gives $4\pi M_{eff}$ (= $4\pi M_s$, when there is no magnetic anisotropy). Form the slope the gyromagnetic ratio, $\gamma = g\mu_B/h$, allows us to determine the Lande g-factor, g = 2.35 and M_{eff} = 1,050 emu/cm^3.

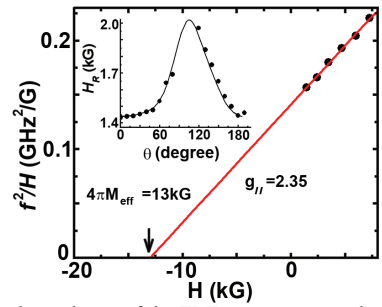

FIGURE 2. Frequency dependence of the FMR resonance peak with the magnetic field applied in the plane of the substrate surface. The inset shows the resonance field H_R as a function of the angle between the B field and the plane of the substrate.

Inset in Fig. 2 shows the data of FMR experiments with the field applied at different angles with respect to the surface of the sample. The resonance field increases as the angle changes from 0° to 90°, indicative of an extended ferromagnetic film-like structure embedded inside the silicon.

DISCUSSIONS AND CONCLUSIONS

SQUID measurements confirmed that as-implanted S-1 sample showed a strong magnetic ordering, while the annealed S-2 sample showed no magnetic interactions. It is quite reasonable to assume that implantation induced defects could very likely increase the concentration of the unpaired electrons in the silicon sample. Annealing tends to decrease the concentration of unpaired electrons. The fact that sample S-1 showed no FMR signal at room temperature, while showing magnetic behavior at low temperature, may indicate that the magnetization in this sample is generated in localized and diluted clusters, which will not resonate collectively upon application of microwave radiation.

In addition, the FMR response observed in sample α-3 may indicate that annealing of the samples damaged with α-particles is critical to form extended ferromagnetic thin film structures within the silicon. The fact that samples α-1 and α-2 did not show FMR response suggests that the annealing temperature and time are crucial to obtain defect-induced ferromagnetism in silicon samples.

ACKNOWLEDGMENTS

L.C. wishes to acknowledge the partial financial support from Apollo Technologies, Inc. and Florida High Tech Corridor Research Program.

REFERENCES

1. T. Dubroca, R.E. Hummel, and A. Angerhofer, Appl. Phys. Lett. **88**, 182504 (2006).
2. J. Hack, M.H. Ludwig, W. Geerts, and R.E. Hummel, Mater. Res. Soc. Symp. Proc. **452**, 147 (1997).
3. M. Bolduc et al., Phys. Rev. B **71** 033302 (2005).
4. A. Misiuk, L. Chow, A. Barcz, B. Surma, J. Bak-Misiuk, P. Romanowski, W. Osinniy, F. Salman, G. Chai, M. Prujszczyk, A. Trojan, in: High Purity Silicon 9, Eds: C.L. Claeys, R. Falster, M. Watanabe, P. Stallhofer, Pennington 2006, pp. 481.
5. S. Zhou, K. Potzger, G. Zhang, A. Mucklich, F. Eichhorn, N. Schell, R. Grotzschel, B. Schmidt, W. Skorupa, M. Helm, J. Fassbender, and D. Geiger, Phys. Rev. B **75**, 085203 (2007).
6. A. Misiuk et al., J. Alloys Comp. **423**, 201-204 (2006).
7. A.F. Khokhlov and P. V. Pavlov, JETP Lett. **24**, 211-213 (1976).
8. S.V. Adashkevich et al., JETP Lett. **84**, 547-550 (2007).
9. R. Laiho, E. Lahderanta, L. Vlasenko, M. Vlasemko, and M. Afanasiev, J. Lumin. **57**, 197-200 (1993).
10. T.L. Makarova, Semiconductors, **38**, 615-638 (2004).
11. Y.M. Shulga, A.I. Boldyrev, and A.A. Ovchinnikev, Chem. Phys. Lett. **189**, 577-580 (1992).
12. E. Esquinazi,R. Hohne, K.H. Han et. al, Carbon, 42, 1213, (2004).
13. T. L. Makarova, B. Sundqvist, P. Esquinazi et al, Nature, **413**, 716-718 (2001).
14. P. Zhang, F. Stevie , R. Vanfleet, R. Neelakantan, M. Klimov, D. Zhou, and L. Chow, J. Appl. Phys. **96**, 1053-1058 (2004).
15. L. Chow, A. Misiuk, et al, J. Mater Sci: Mater Electron, DOI 10.1007/sI0854-007-9481-4.
16. C. Kittel, *Introduction to Solid State Physics, 7th ed.* Wiley, New York, 1996.